Scripta Materialia 109 (2015) 1–5

Contents lists available at ScienceDirect

Scripta Materialia

journal homepage: www.elsevier.com/locate/scriptamat

Viewpoint Paper

# Recent progress in hydrogen-rich materials from the perspective of bonding flexibility of hydrogen

Shigeyuki Takagi [a,*], Shin-ichi Orimo [a,b]

[a] Institute for Materials Research, Tohoku University, Sendai 980-8577, Japan
[b] WPI-Advanced Institute for Materials Research, Tohoku University, Sendai 980-8577, Japan

ARTICLE INFO

*Article history:*
Received 17 June 2015
Accepted 19 July 2015

*Keywords:*
Hydrides
Hydrogen storage
Electronic structure
First-principles calculations

ABSTRACT

The bonding flexibility of hydrogen is a source of various interesting functionalities in hydrides. Here, we illustrate the benefits of this flexibility through several selected examples of recent progress in the development of hydrogen storage materials. From the viewpoint of electronegativity, we discuss the diverse cohesion and materials science underlying the bonding flexibility of hydrogen in hydrides.



## 1. Introduction

Hydrogen, although having only one electron, exhibits an exceptionally rich chemistry, forming various chemical bonds in materials. For an intuitive understanding, Fig. 1 illustrates such a bonding flexibility of hydrogen with a tetrahedral diagram (hereafter, "hydrogen diagram"). The spheres occupying each vertex of the diagram represent four ideal chemical-bonding states in which hydrogen occurs: (i) interstitial hydrogen ($H^0$, ~0.53 Å in radius [1]) dissolved in the metal lattices, (ii) proton ($H^+$, ~0 Å in radius [2]) normally found in acids, (iii) hydride ion ($H^-$, 1.4–2.1 Å in radius [1,3]), as in the perovskite hydrides, and (iv) covalently bonded hydrogen ($H^{cov.}$, ~0.37 Å in radius [4]), as in the complex hydrides.

In actual materials, hydrogen occurs in intermediate states away from the vertices. A good example is the perovskite hydride $LiNiH_3$, which possesses a metallic electronic structure in which substantial hybridization occurs between the Ni *spd* and H 1*s* states [5,6], even though the ideal perovskite structure is normally observed in ionic hydrides. In this case, hydrogen would occur at the edge between $H^-$ and $H^{cov.}$ in the hydrogen diagram. In addition, several materials that contain multiple hydrogen atoms with obviously different chemical-bonding states exist [7–12]. For instance, the complex transition-metal hydride $Na_2Mg_2FeH_8$ contains two $H^-$ ions in addition to a transition-metal hydride complex, $[FeH_6]^{4-}$, whose cohesion is dominated by covalent interactions ($H^{cov.}$) [10]. In this case, the two types of hydrogen would appear separately in the diagram. As such, the hydrogen diagram covers all such flexible chemical-bonding states.

The bonding flexibility of hydrogen leads to various functionalities in hydrides, including hydrogen storage [7,10,13–17], fast ionic conductivity [18–23], superconductivity [24–28], magnetism [29,30], and metal–insulator transition [8,31]. The monovalency of the $H^-$ ion provides tunability of the charge state when incorporated into materials or substituted for elements with different valence charge states. This tunability enables the inclusion of a wider variety of cations, thereby enabling tuning of material properties, such as hydrogen dissociation temperature [10,11] and the occurrence of spin ordering [29]. The high solubility of monoelectronic $H^0$ in metals allows the fine tuning of the electron count, leading to a drastic change in the optical properties of host materials [8,31]. In particular, the recent discovery of a 190-K superconducting phase in hydrogen sulfide under compression [30] has led to a renewed interest in hydrogen-rich materials [27,28]. In these materials, a large amount of hydrogen would have already undergone a form of chemical precompression, leading to metallization at a pressure much lower than that predicted for pure hydrogen [24].

Besides the technological importance of hydrides, there is also a considerable scientific interest in unraveling their diverse cohesion. A key to the flexibility of hydrogen would be the specific electronegativity, which is of average magnitude among all the elements, leading to a drastic change in the chemical-bonding states depending on which elements hydrogen interacts with and on the presence of even small perturbations. In turn, the specific

* Corresponding author.
*E-mail address:* shigeyuki.takagi@imr.tohoku.ac.jp (S. Takagi).

http://dx.doi.org/10.1016/j.scriptamat.2015.07.024
1359-6462/

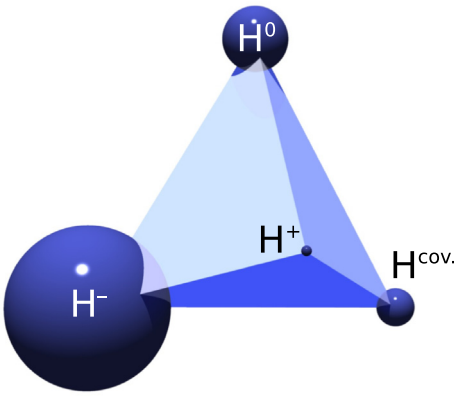


**Fig. 1.** Hydrogen diagram. This diagram illustrates the bonding flexibility of hydrogen with a tetrahedron; the spheres located at each vertex represent a proton ($H^+$), a hydride ion ($H^-$), covalently bonded hydrogen ($H^{cov.}$) and neutral hydrogen ($H^0$).

electronegativity of hydrogen causes difficulty in quantitatively understanding the chemical bonding related to hydrogen and thereby often provokes controversy [32–35].

In this Viewpoint, recent progress in the development of hydrogen storage materials is taken as an example to explain the benefits of the bonding flexibility of hydrogen. We then discuss the diverse cohesion in hydrides and the materials science underlying this flexibility from the viewpoint of electronegativity.

## 2. Recent progress in solid-state hydrogen storage

Solid-state hydrogen storage is divided into several classes according to the storage medium used. A prototypical medium is metallic hydrides, such as $TiFeH_2$, in which hydrogen interstitially dissolves into the metal lattices, primarily as $H^0$. Some of these materials exhibit very promising properties, such as fast reaction kinetics, reversible hydrogen uptake/release under modest temperature and pressure conditions, and high volumetric hydrogen capacity; however, their gravimetric hydrogen capacities are insufficient for automotive applications [36] (e.g., the US Department of Energy's system target for 2017 is 5.5 mass% [37], which is much higher than the 1.9 mass% of $TiFeH_2$ alone).

Among the methods spanning many approaches, one involving the use of complex transition-metal hydrides has a clear advantage in volume and weight efficiencies and has thus attracted attention for many years. The major disadvantage of this method is the high hydrogen dissociation temperature that arises from the high thermodynamic stability of the complex transition-metal hydrides, which makes reversible room-temperature applications challenging. For example, dimagnesium iron(II) hydride ($Mg_2FeH_6$), which is composed of only abundant elements, reversibly stores 150 kg $H_2/m^3$ and 5.5 mass% of hydrogen; however, its operating temperature reported is approximately 773 K [38].

The complex transition-metal hydrides used as the storage medium in this method refer to the insulating hydrides that contain homoleptic transition-metal hydride complexes such as $[FeH_6]^{4-}$ [7,13,39]. The ligand-field effects play a key role in the formation of the hydride complexes [10,12,40–43], as discussed in detail below.

Fig. 2 shows a schematic for the formation of the electronic structure of a prototypical complex transition-metal hydride, $Mg_2FeH_6$, from energy levels of the constituent elements (note that this material consists of two magnesium atoms and an $FeH_6$ structural unit, in which the iron atom is octahedrally coordinated by six hydrogen atoms). In the octahedral H ligand field with $O_h$ point-group symmetry, the Fe 3*d*, 4*s*, and 4*p* orbitals hybridize with H 1*s* orbitals ($sp^3d^2$ hybridization), forming six bonding states (nondegenerate $a_{1g}$, threefold degenerate $t_{1u}$, and twofold degenerate $e_g$ symmetry states), three nonbonding states (threefold degenerate $t_{2g}$ symmetry states) and the corresponding antibonding states ($a_{1g}^*$, $t_{1u}^*$, and $e_g^*$ symmetry states). All of the bonding and nonbonding states are fully occupied by the eighteen electrons, and the Fermi level falls in the gap between nonbonding and antibonding states. The electropositive Mg orbitals occur further above the antibonding states and thus donate a total of four electrons to the $FeH_6$ unit. As such, the cohesion of the $FeH_6$ unit is dominated by the Fe-H covalent interactions stabilized by the charge transfer from electropositive Mg, leading to high thermodynamic stability in this material. On the basis of hydrogen diagram in Fig. 1, the six hydrogen atoms forming the hydride complexes can primarily be understood as $H^{cov.}$.

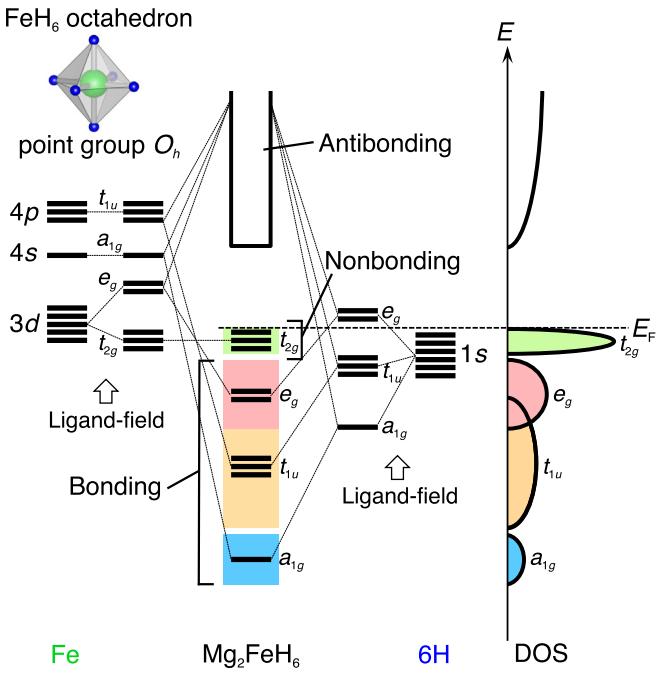


**Fig. 2.** Schematic of the formation of the electronic structure of $Mg_2FeH_6$ from the energy levels of the Fe 3*d*, Fe 4*s*, Fe 4*p*, and H 1*s* orbitals in the octahedral ligand field with $O_h$ point group symmetry.

From the electronic structure viewpoint, one expects that the thermodynamic stability of $Mg_2FeH_6$ can be tuned through modifying the covalent interactions in the hydride complexes by altering the charge transferability of counterions, i.e., by cation selection. In this context, Miwa et al. theoretically examined the correlation between the cation electronegativity and the thermodynamic stability in a series of $(M,M')_2[FeH_6]^{4-}$ complex transition-metal hydrides in which two Mg atoms in $Mg_2FeH_6$ are substituted by the various elements with different electronegativities [17], similar to the approach Nakamori et al. used to investigate a series of $M(BH_4)_x^-$ borohydrides [14].

The black open circles in Fig. 3 show the standard heats of formation of complex transition-metal hydrides $(M,M')_2FeH_6$ as a function of the cation electronegativity on the Allred-Rochow scale [44]. As expected from the bonding scheme, a linear correlation between them is clearly observed; i.e., the thermodynamic stability of $Mg_2FeH_6$ can be tuned by substitution of Mg with elements having different electronegativities.

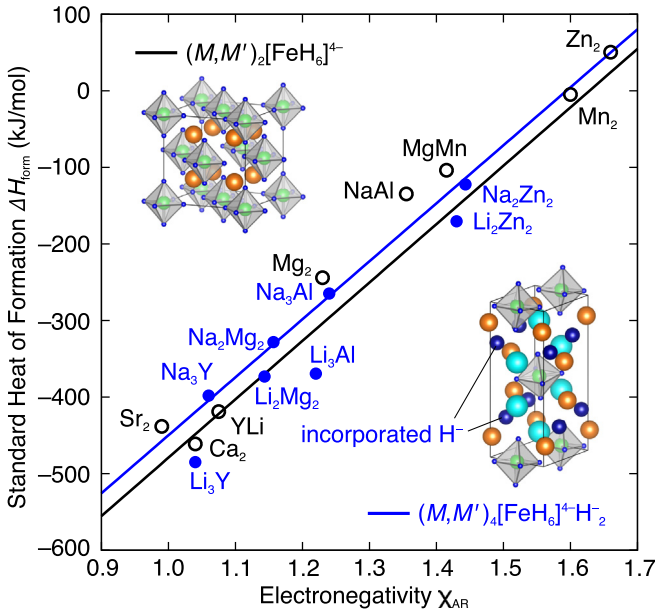


**Fig. 3.** Standard heat of formation $\Delta H_{form}$ as a function of cation electronegativity on the Allred-Rochow scale $\chi_{AR}$ for two types of complex transition-metal hydrides $(M,M')_2[FeH_6]^{4-}$ and $(M,M')_4[FeH_6]^{4-}H_2^-$. A valency-averaged electronegativity was used for mixed-cation systems. The standard heats of formation for $(M,M')_2[FeH_6]^{4-}$ and $(M,M')_4[FeH_6]^{4-}H_2^-$ were taken from Refs. [17,10], respectively. Solid lines denote least-squares fits to the results. (For interpretation of the references to colour in this figure legend, the reader is referred to the web version of this article.)

Although this correlation provides a useful insight into the rational design of new complex transition-metal hydrides, the tunability of the thermodynamic stability is practically limited to some extent because of a small number of possible combinations of cations to compensate the tetravalent charge state of the $[FeH_6]^{4-}$ anion. One strategy for increasing these combinations is to increase the total anionic charge state [42]. For this purpose, we here introduce a novel method for increasing the charge state by incorporating $H^-$ ions into complex transition-metal hydrides [10], as depicted in Fig. 4.

The blue solid circles in Fig. 3 show the standard heats of formation of $(M,M')_4FeH_8$, which is composed of an $[FeH_6]^{4-}$ anion, two incorporated $H^-$ ions, and a total of four cations that compensate the hexavalent anionic charge state, as a function of cation electronegativity. As evident in the figure, we observed a correlation between the cation electronegativity and the standard heat of formation in the complex transition-metal hydrides with a hexavalent anionic charge state formed by the $[FeH_6]^{4-}$ anion and the two incorporated $H^-$ ions; this correlation is similar to that observed in the case of $(M,M')_2FeH_6$ with a tetravalent anionic charge state. Thus, the increased number of combinations of cations resulting from the incorporation of $H^-$ ions enhances the tunability of the thermodynamic stability.

To summarize the discussion thus far, the bonding flexibility of hydrogen contributes to the modification of the thermodynamic stability of complex transition-metal hydrides in two ways: (i) as $H^{cov.}$, where the covalent interactions with the coordination center are tuned by charge transfer from counterions, or (ii) as $H^-$, which enhances the tunability of thermodynamic stability through increasing the combinations of countercations. These findings will be beneficial in obtaining materials with optimal stability for reversible room-temperature hydrogen storage applications. Notably, the incorporation of $H^-$ ions also effectively increases the hydrogen content, e.g., the gravimetric hydrogen density of the hypothetical $Li_3AlFeH_8$ studied in Ref. [10] reaches 7.2 mass%, which is approximately 30% higher than that of $Mg_2FeH_6$ and would be the highest reported density for a complex transition-metal hydride (cf. 6.7 mass% for $Li_4FeH_6$ [45,46]), if this material can be synthesized.

## 3. Materials science underlying the flexibility of hydrogen

Since Pauling proposed the concept of electronegativity [47], the electronegativity difference (ΔEN) has been widely used to classify heteroatomic chemical bonding, although it has been recognized to provide only an approximate division. In general, the heteroatomic bonds with ΔEN less than 1.7 on the Pauling scale are characterized as predominantly covalent, whereas the others are described as predominantly ionic.

Sproul proposed a new method of classification that involves the use of a two-dimensional plot of lower electronegativity vs. higher electronegativity in the heteroatomic bonds [48], instead of ΔEN, as shown in Fig. 5. The basic idea of this approach is to avoid any information loss by using both the electronegativities as they are (note that the conversion of two electronegativities into ΔEN causes a loss of half of the inherent information). This method

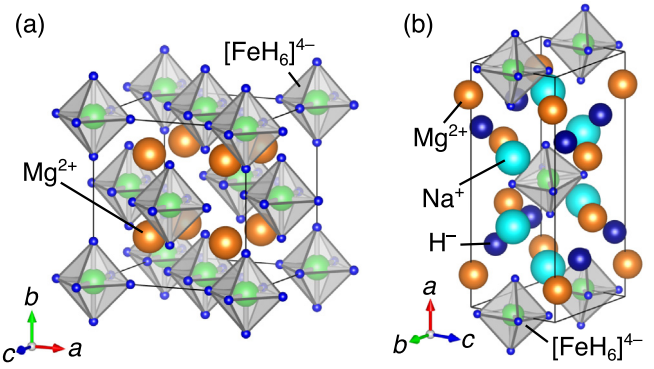


**Fig. 4.** Crystal structure of typical complex transition-metal hydrides (a) $Mg_2FeH_6$ and (b) $Na_2Mg_2FeH_8$ containing two incorporated $H^-$ ions.

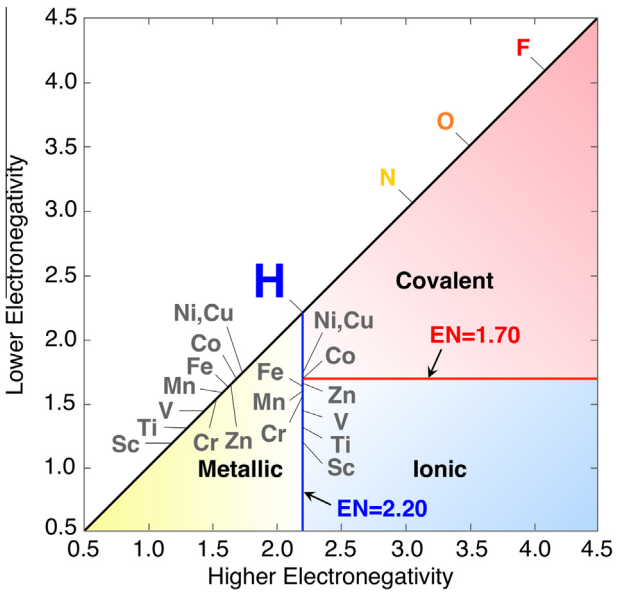


**Fig. 5.** Two-dimensional plot of the electronegativities of two elements forming heteroatomic bonds proposed by Sproul [48]. The electronegativities of representative elements on the Allred-Rochow scale are shown.

successfully divides the representative 312 binary compounds whose bond type is well known into covalent, ionic, and metallic compounds, with only a 4% overall error (the conventional ΔEN causes a 16% error). Briefly, according to this method, the binary compounds with a higher electronegativity less than 2.20 are characterized as having metallic character, whereas the remaining compounds are divided into covalent and ionic compounds, depending on whether the lower electronegativity is greater than 1.70, respectively. It should be emphasized that the boundary of metallic, ionic, and covalent compounds lies on the vertical line with a higher electronegativity value of 2.20, corresponding exactly to that of hydrogen, as shown in Fig. 5. Accordingly, when hydrogen forms heteroatomic bonds with the more electropositive elements, this method cannot classify their bonding character. Thus, the specific electronegativity of hydrogen provides bonding flexibility and, in turn, causes the difficulty in quantitative classification of the chemical bonding in hydrides.

The flexibility and difficulty in quantification appear prominently in the interactions between hydrogen and transition-metal elements. The electronegativity of transition metals is lower than that of hydrogen; therefore, all of the conceivable bonds extend along the vertical line at higher electronegativity EN = 2.2 in Fig. 5. Taking a series of 3*d* transition metals as an example, the electronegativity gradually increases from 1.20 (Sc) to 1.75 (Ni and Cu) when going from left to right along a period and steps over the value of 1.70 that divides the covalent and ionic characters (horizontal line with lower electronegativity at EN = 1.7 in Fig. 5) at Group 9 (Co, whose electronegativity is 1.70) on the Allred-Rochow scale [44]. Thus, on the basis of Fig. 5, the chemical bonding between hydrogen and 3*d* transition metals can be divided into ionic/metallic and covalent/metallic characters according to whether the transition metal is located on the left or right side of Co in the periodic table, respectively. This prediction differs somewhat from experimental observations, as follows.

Whereas the early transition metals in Groups 3–5 form binary metal hydrides, in which hydrogen exists as $H^-$ (ionic) or $H^0$ (metallic), the others, except for palladium, do not form any stable binary hydrides under ambient conditions (i.e., the hydride gap [49]). Meanwhile, the elements belonging to the hydride gap form a varied set of transition-metal hydride complexes with H coordination modes ranging from fourfold to sevenfold [7,12], as schematically depicted in Fig. 6. Thus, the experimental observations indicate that the boundary between ionic/metallic and covalent characters lies between vanadium and chromium.

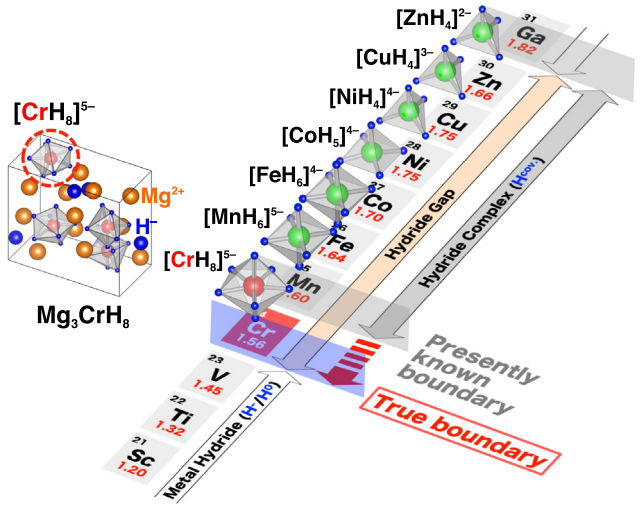


**Fig. 6.** Schematic image of the interaction between hydrogen and the 3*d* transition-metal elements. The discovery of the first Group 6 hydride complex $[CrH_7]^{5-}$ in $Mg_3CrH_8$ indicates that the true boundary for the formation of transition-metal hydride complexes lies between Groups 5 and 6.

This discrepancy could be a consequence of the ligand-field effects in hydride complexes, which promote the structure-dependent hybridization between the H 1*s* and transition-metal *spd* states, leading to enhanced covalency, as previously discussed. For example, from an electronegativity viewpoint, the Fe-H and Mn-H bonds should be classified as ionic/metallic; however, they are actually dominated by covalent interactions in the hydride complexes $[FeH_6]^{4-}$ [17,10] and $[MnH_6]^{5-}$ [40,41], respectively. Furthermore, we recently reported that the pentagonal-bipyramidal H ligand field with $D_{5h}$ point-group symmetry allows the formation of strong $\sigma$-bonds between hydrogen and Group 6 element chromium in $[CrH_7]^{5-}$, which demonstrates that the true boundary for the formation of homoleptic transition-metal hydride complexes, i.e., $H^{cov.}$, lies between Groups 5 and 6 [12], as shown in Fig. 6.

As previously discussed, the chemical bonds between hydrogen and transition-metals extend exactly on the boundary that divides metallic, ionic, and covalent characters; therefore, even small perturbations, such as the aforementioned structure-dependent hybridization induced by ligand-field effects, significantly affect the classification. This situation is quite different from those for other typical electronegative elements such as nitrogen, oxygen, and fluorine. In the case of oxygen, for example, the long-range Coulomb interaction in solids primarily stabilizes the $O^{2-}$ ion in metal oxides, although modest covalent contributions may exist. Given such a situation, the structural information, such as the H coordination modes (coordination number and point-group symmetry) must be considered, at least in the quantitative understanding of chemical bonding in hydrides.

## 4. Summary and conclusions

In this Viewpoint, we attempted to highlight both the technological importance and scientific interest in bonding flexibility of hydrogen in hydrogen-rich materials, which we illustrated with several selected examples of recent progress in the development of hydrogen storage materials. In these materials, the bonding flexibility plays a key role both in tuning the thermodynamic stability strongly related to the hydrogen dissociation temperature and in achieving greater hydrogen contents. We discussed the materials science underlying the bonding flexibility on the basis of the successful Sproul's method and demonstrated that the specific electronegativity of hydrogen provides its flexibility and, in turn, causes the difficulty in quantitatively understanding the cohesion in hydrides.

Chemical bonding is essentially a source of various properties of condensed matter. Given the diverse cohesion in hydrides, as demonstrated in "hydrogen diagram", hydrogen-rich materials are likely to exhibit novel functionalities and must therefore be further explored. We hope the current discussion is useful in the development of novel hydrogen-rich materials.

## Acknowledgements

We are grateful for helpful discussions with Dr. K. Miwa and the use of supercomputing resources at the Center for Computational Materials Science of the Institute for Materials Research, Tohoku University. This work was supported by JSPS KAKENHI (grant numbers 26820312 and 25220911).

## References


[1] Y. Fukai, The Metal-Hydrogen System, 2nd Edition., Springer-Verlag, Berlin, 2005.
[2] V. Schomaker, D.P. Stevenson, Rev. Mod. Phys. 84 (2012) 1527–1605.
[3] A. Bouamrane, J.P. Lavel, J.P. Soulie, J.P. Bastide, Mater. Res. Bull. 35 (2000) 545–549.
[4] V. Schomaker, D.P. Stevenson, J. Am. Chem. Soc. 63 (1941) 37–40.
[5] S. Takagi, H. Saitoh, N. Endo, R. Sato, T. Ikeshoji, M. Matsuo, K. Miwa, K. Aoki, S. Orimo, Phys. Rev. B 87 (2013) 125134.
[6] R. Sato, H. Saitoh, N. Endo, S. Takagi, M. Matsuo, K. Aoki, S. Orimo, Appl. Phys. Lett. 102 (2013) 091901.
[7] K. Yvon, CHIMIA 52 (1998) 613–619.
[8] K. Yvon, G. Renaudin, C.M. Wei, M.Y. Chou, Phys. Rev. Lett. 94 (2005) 066403.
[9] K. Kadir, D. Noréus, Inorg. Chem. 46 (2007) 2220–2223.
[10] S. Takagi, T.D. Humphries, K. Miwa, S. Orimo, Appl. Phys. Lett. 104 (2014) 203901.
[11] T.D. Humphries, S. Takagi, G. Li, M. Matsuo, T. Sato, M.H. Srby, S. Deledda, B.C. Hauback, S. Orimo, J. Alloys Compd. Complex transition metal hydrides incorporating ionic hydrogen: Synthesis and characterization of $Na_2Mg_2FeH_8$ and $Na_2Mg_2RuH_8$ (in press) http://dx.doi.org/10.1016/j.jallcom.2014.12.113.
[12] S. Takagi, Y. Iijima, T. Sato, H. Saitoh, K. Ikeda, T. Otomo, K. Miwa, T. Ikeshoji, K. Aoki, S. Orimo, Angew. Chem. Int. Ed. 54 (2015) 5650–5653.
[13] W. Bronger, Angew. Chem. Int. Ed. 30 (1991) 759–768.
[14] Y. Nakamori, K. Miwa, A. Ninomiya, H. Li, N. Ohba, S. Towata, A. Züttel, S. Orimo, Phys. Rev. B 74 (2006) 045126.
[15] S. Orimo, Y. Nakamori, J.R. Eliseo, A. Züttel, C.M. Jensen, Chem. Rev. 107 (2007) 4111–4132.
[16] H. Saitoh, S. Takagi, N. Endo, A. Machida, K. Aoki, S. Orimo, Y. Katayama, APL Mater. 1 (2013) 032113.
[17] K. Miwa, S. Takagi, M. Matsuo, S. Orimo, J. Phys. Chem. C 117 (2013) 8014–8019.
[18] M. Matsuo, Y. Nakamori, S. Orimo, Appl. Phys. Lett. 91 (2007) 224103.
[19] M. Matsuo, S. Orimo, Adv. Energy Mater. 1 (2011) 161–172.
[20] T. Ikeshoji, Y. Ando, M. Otani, E. Tsuchida, S. Takagi, M. Matsuo, S. Orimo, Appl. Phys. Lett. 103 (2013) 133903.
[21] T. Ikeshoji, E. Tsuchida, S. Takagi, M. Matsuo, S. Orimo, RSC Adv. 4 (2014) 1366–1370.
[22] A. Unemoto, M. Matsuo, S. Orimo, Adv. Funct. Mater. 24 (2014) 2267–2279.
[23] T.J. Udovic, M. Matsuo, W.-S. Tang, H. Wu, V. Stavila, A.V. Soloninin, R.V. Skoryunov, O.A. Babanova, A.V. Skripov, J.J. Rush, A. Unemoto, H. Takamura, S. Orimo, Adv. Mater. 26 (2014) 7622–7626.
[24] N.W. Ashcroft, Phys. Rev. Lett. 92 (2004) 187002.
[25] M.I. Eremets, I.A. Trojan, S.A. Medvedev, S.J. Tse, Y. Yao, Science 319 (2008) 156–1509.
[26] S. Iimura, S. Matuishi, H. Sato, T. Hanna, Y. Murabe, S.-W. Kim, J.-E. Kim, M. Takata, H. Hosono, Nat. Commun. 3 (2012) 943.
[27] H. Zhang, X. Jin, Y. Lv, Q. Zhuang, Y. Liu, Q. Lv, K. Bao, D. Li, B. Li, T. Cui, Sci. Rep. 5 (2015) 8845.
[28] Y. Li, J. Hao, H. Liu, J.S. Tse, Y. Wang, Y. Ma, Sci. Rep. 5 (2015) 9948.
[29] C. Tassel, Y. Goto, Y. Kuno, J. Hester, M. Green, Y. Kobayashi, H. Kageyama, Angew. Chem. Int. Ed. 53 (2014) 10377–10380.
[30] A.P. Drozdov, M.I. Eremets, I.A. Trojan, arXiv:1412.0460.
[31] J.N. Huiberts, R. Griessen, J.H. Rector, R.J. Wijingaarden, J.P. Dekker, D.G. de Groot, N.J. Koeman, Nature 380 (1996) 231–234.
[32] P. Vajeeston, P. Ravindran, A. Kjekshus, H. Fjellåg, Phys. Rev. B 69 (2004) 020104(R).
[33] A. Aguayo, D.J. Singh, Phys. Rev. B 69 (2004) 155103.
[34] D.J. Singh, Phys. Rev. B 71 (2015) 216101.
[35] P. Vajeeston, P. Ravindran, A. Kjekshus, H. Fjellåg, Phys. Rev. B 71 (2005) 216102.
[36] L. Schlapbach, A. Züttel, Nature 414 (2001) 353–358.
[37] See http://energy.gov/eere/fuelcells/hydrogen-storage-current-technology for DOE targets for On-board hydrogen storage system.
[38] B. Bogdanović, A. Reiser, K. Schlichte, B. Soliethoff, B. Teche, J. Alloys Compd. 1–2 (2002) 77–89.
[39] J.J. Didisheim, P. Zolliker, K. Yvon, P. Fischer, J. Shefer, M. Gubelmann, A.F. Williams, Inorg. Chem. 23 (1984) 1953.
[40] M. Matsuo, K. Miwa, S. Semboshi, H.-W. Li, M. Kano, S. Orimo, Appl. Phys. Lett. 98 (2011) 221908.
[41] S. Takagi, K. Miwa, T. Ikeshoji, M. Matsuo, M. Kano, S. Orimo, Appl. Phys. Lett. 100 (2012) 021908.
[42] S. Takagi, K. Miwa, T. Ikeshoji, R. Sato, G. Li, K. Aoki, S. Orimo, J. Alloys Compd. 580 (2013) S274–S277.
[43] S. Takagi, T. Ikeshoji, M. Matsuo, T. Sato, H. Saitoh, K. Aoki, S. Orimo, Appl. Phys. Lett. 103 (2013) 113903.
[44] A.L. Allred, E.G. Rochow, J. Inorg. Nucl. Chem. 5 (1958) 264–268.
[45] S. Takagi, T. Ikeshoji, T. Sato, K. Aoki, S. Orimo, J. Japan Inst. Met. Mater. 77 (2013) 604–608 (in Japanese).
[46] H. Saitoh, S. Takagi, M. Matsuo, Y. Iijima, N. Endo, K. Aoki, S. Orimo, APL Mater. 2 (2014) 076103.
[47] L. Pauling, The Nature of the Chemical Bond, 3rd Edition., Cornell University Press, Ithaca, NY, 1967.
[48] G. Sproul, J. Chem. Edu. 78 (1994) 387–390.
[49] A. Züttel, Mater. Today 6 (2003) 24–33.